



Published in final edited form as:

Leukemia. 2020 February ; 34(2): 380–390. doi:10.1038/s41375-019-0566-x.

Inhibition of *Slug* effectively targets leukemia stem cells via the Slc13a3/ROS signaling pathway

Zhonghui Zhang^{1,4}, Lei Li², Chen Wu¹, Guoshu Yin^{3,4}, Pei Zhu⁴, Yalu Zhou⁴, Yuanfan Hong⁴, Hongyu Ni⁵, Zhijian Qian⁶, Wen-Shu Wu^{4,*}

¹School of Life Sciences, Shanghai University, Shanghai, 200444, China

²Department of Pediatrics, Union Hospital, Tongji Medical College, Huazhong University of Science and Technology, Wuhan, 430022, China

³Department of Endocrinology and Metabolism, The First Affiliated Hospital of Shantou University Medical College, Shantou, Guangdong, 515041, China

⁴Division of Hematology/Oncology, Department of Medicine and University of Illinois Cancer Center, University of Illinois at Chicago, IL 60612, USA

⁵Department of Pathology, University of Illinois at Chicago, IL 60612, USA

⁶Division of Hematology/Oncology, Department of Medicine and The University of Florida Cancer/Genetics Research Complex, FL 32610, USA

Abstract

Leukemia stem cells (LSCs) are rare populations of acute myeloid leukemia (AML) cells that are able to initiate, maintain and propagate AML. Targeting LSCs is a promising approach for preventing AML relapse and improving long-term outcomes. While *Slug*, a zinc-finger transcription repressor, negatively regulates the self-renewal of normal hematopoietic stem cells, its functions in AML are still unknown. We report here that *Slug* promotes leukemogenesis and its loss impairs LSC self-renewal and delays leukemia progression. Mechanistically, *Slc13a3*, a direct target of *Slug* in LSCs, restricts the self-renewal of LSCs and markedly prolongs recipient survival. Genetic or pharmacological inhibition of *SLUG* or forced-expression of *Slc13a3* suppresses the growth of human AML cells. In conclusion, our studies demonstrate that *Slug* differentially regulate self-renewal of LSCs and normal HSCs, and both *Slug* and *Slc13a3* are potential therapeutic targets of LSCs.

Users may view, print, copy, and download text and data-mine the content in such documents, for the purposes of academic research, subject always to the full Conditions of use:http://www.nature.com/authors/editorial_policies/license.html#terms

*To whom correspondence should be addressed: wenshuwu@uic.edu, Phone: 312-996-2586, Fax: 312-413-4131.

AUTHOR CONTRIBUTIONS

Contribution: Z.Z. and W.S.W. were responsible for experimental design and data analysis; Z.Z., L.L., C.W., G.Y., P.Z., and Y.H. performed experiments; Y.Z. performed microarray analyses; Z.Z. and W.S.W. wrote the manuscript; Z.Q. and N.H. provided key materials and suggestions for experimental design; W.S.W. provided supervision.

CONFLICT OF INTEREST

The authors declare no conflict of interest.

INTRODUCTION

Acute Leukemia, including acute lymphoblastic leukemia (ALL) and acute myeloid leukemia (AML), is an aggressive and lethal blood cancer afflicting people of all ages^{1, 2}. Although the 5-year survival rate for some subtypes of ALL patients under the age of 15 has achieved a high cure rate (~80%), the 5-year overall survival rate for AMLs is still only ~40%³⁻⁶. AML has been traditionally characterized as a cell autonomous disorder resulting from genetic mutations in hematopoietic stem cells (HSCs) or committed progenitor compartments^{7, 8}. The MLL gene, located at human chromosome 11 band q23 (11q23), is frequently involved in chromosome translocation and gives rise to a chimeric transcript consisting of 5' MLL and 3' sequences of a partner gene. Most frequently, MLL rearrangements are MLL-AF4, MLL-AF6, MLL-AF9, MLL-AF10 and MLL-ENL⁹, which are found in ~10% of human leukemia¹⁰.

Leukemia stem cells (LSCs), a rare subpopulation of AML cells with limitless self-renewal potential and differentiation block, are capable of initiation, maintenance, and serial propagation of AMLs. Targeting LSCs has been considered as a key therapeutic strategy for AML relapse and long-term outcomes of AML clinical therapy. Self-renewal of LSCs is involved in activation of numerous signaling pathways including HoxA cluster, Wnt-beta-catenin, telomerase activation, NF- κ B, and mTOR/PI3K/PTEN^{6, 7, 11-14}.

Slug/Snail2, a zinc-finger transcriptional repressor, is a highly conserved Slug/Snail family of transcriptional factors found in diverse species¹⁵. Slug/Snail2 is involved in many important biological regulation processes, such as epithelial-mesenchymal transition (EMT), mammary stem cell activity, cancer metastasis, and cellular reprogramming¹⁶⁻¹⁹. Previous studies report that Slug is specifically expressed in t (17;9) (q22;p13) leukemic cells²⁰. Transgenic mice expressing Slug develop mesenchymal tumors (leukemia and sarcomas)²¹. Our recent studies show that Slug deficiency enhances self-renewal of HSCs during hematopoietic regeneration through a novel negative-feedback regulatory loop in the SCF/c-Kit signaling pathway^{15, 22}. However, the roles of Slug in LSC initiation and maintenance and therapeutic capacity of AML are still unknown.

In the present study, we investigated roles of Slug in LSC initiation and maintenance in MLL-AF9-induced leukemia and potential therapeutics for human AML cells. We demonstrated that SLUG is highly expressed in bone marrow, peripheral blood, and L-GMPs of human AML patients. Slug deficiency delays MLL-AF9 mediated leukemia onset by reducing cycling LSCs and promoting LSC apoptosis. Suppression of Slug expression impaired the maintenance of LSCs. Using microarray analysis, we found that endogenous Slc13a3 (also called NaDC3, a Na⁺/dicarboxylate cotransporter) is highly elevated in Slug-deficient LSCs compared to wild-type LSCs. By quantitative PCR (qPCR) analysis, chromatin immunoprecipitation (ChIP) assay, and colony-forming assay, we established Slc13a3 as a direct target gene of Slug in leukemogenesis. Consistently, overexpression of Slc13a3 reduced the colony number *in vitro*, decreased the frequency of LSCs, and delayed mouse AML progression *in vivo*. Slug/Slc13a3 signaling pathway enhances intracellular reactive oxygen species (ROS) level and ROS inhibitor N-acetyl-L-cysteine (NAC) attenuates the roles of Slug and Slc13a3 in leukemia progression by regulation of cell cycle

and apoptosis of LSCs. Furthermore, using inducible inhibition shRNA system and TAT-SNAG (a cell-permeable peptide corresponding to the SNAG domain of SLUG), we showed that genetic inhibition or pharmacological targeting of SLUG impairs human AML cell growth. Meanwhile, TAT-SNAG dramatically enhances cytotoxic effects of cytarabine on human AML cells. Similarly, we observed a significant downregulation of SLC13A3 expression in human AML patients, which is positively correlated with SLUG expression. Overexpression of Slc13a3 suppresses human AML cell growth and colony formation *in vitro*. Together, our study provides strong evidence that Slug is essential for the initiation and maintenance of LSCs in MLL-AF9-induced leukemia and demonstrates that Slug and Slc13a3 are potential therapeutic targets for LSCs.

MATERIALS AND METHODS

Mice

C57BL/6 and C57/6.SJL were purchased from the Jackson Laboratory (Bar Harbor, ME, USA). *Slug* knockout mice were generated as described previously and backcrossed to C57BL/6 (CD45.2) background for > 6 generations²⁰. All the animal studies were approved by the Animal Care and Use Committee at Shanghai University and the University of Illinois at Chicago (Approval Number: 16–111).

Additional information can be found in Supplemental Methods.

RESULTS

SLUG expression is elevated in AML patients

Our previous reports showed that *Slug* is selectively expressed in mouse HSCs and myeloid lineages²². To assess the potential clinical relevance of SLUG expression levels in AML patients and in the normal human population, we searched clinical databases online (<http://medicalgenome.kribb.re.kr/GENT/overview.php>) and found that SLUG expression was aberrantly overexpressed in peripheral blood cells of AML patients, bone marrow (BM) cells of FAB (FAB, French-American-British classification) subtype AML-M1, M2, M3, M4, M5 versus normal blood cells and bone marrow cells (Figure 1A, Supplemental Figure 1, Supplemental Table 1). More importantly, the upregulation of SLUG expression was observed in LSCs of AML patients compared to normal GMPs (Supplemental Figure 2). Using quantitative PCR (qPCR), we observed that *Slug* transcription was upregulated in Lin⁻Sca-1⁺ hematopoietic stem and progenitor cells (HSPCs) expressing various oncogenes (MLL-AF9, HoxA9 and Mesi1) (Figure 1B, Supplemental Figure 3). To evaluate the expression levels of *Slug* in LSCs, we also examined an AML mouse model driven by MLL-AF9. *Slug* expression in LSCs (defined as L-GMP, Lin⁻ GFP⁺ c-Kit⁺ CD34⁺ CD16/32⁺) was much higher than that in normal GMPs (Lin⁻ c-Kit⁺ CD34⁺ CD16/32⁺), but similar to that in normal HSCs (Lin⁻ Sca-1⁺ c-Kit⁺ CD150⁺ CD48⁻), suggesting that Slug was downregulated in committed progenitors (i.e. GMP) but reactivated in LSCs (Figure 1C). The data in the AML mouse model were consistent with the results in human AML cells, which suggests that Slug may have an important role in AML.

Slug deficiency impairs self-renewal of LSCs and delays AML onset in murine

AML—In order to determine the role of Slug in AML cells, we enriched Lin⁻Sca-1⁺ HSPCs from *Slug*^{+/+} or *Slug*^{-/-} mice by a single intraperitoneal dose of 5-fluorouracil (5-FU) and then transduced with retroviral MLL-AF9 particles (Figure 2A). *In vitro* colony-forming/replating assays showed that Slug deficiency suppressed MLL-Af9-mediated immortalization of mouse HSPCs (Figure 2B). AML colonies induced by MLL-AF9 are CFU-GM-like colonies. *Slug*^{-/-} AML colonies were characteristically smaller compared to *Slug*^{+/+} AML colonies (Supplemental Figure 4). To examine the roles of Slug for AML *in vivo*, equal numbers of *Slug*^{+/+} or *Slug*^{-/-} MLL-AF9-transduced Lin⁻Sca-1⁺ HSPCs were transplanted into irradiated CD45.1 recipients. Both MLL-AF9-transduced *Slug*^{+/+} and *Slug*^{-/-} HSPCs developed AML with full penetrance in recipient mice; however, *Slug*^{-/-} AML displayed significantly delayed AML onset compared to *Slug*^{+/+} median survival, 77 days vs 57 days, respectively ($P < 0.01$) (Figure 2C, Supplemental Figure 5A). To assess the impact of *Slug* depletion on long-term self-renewal of LSCs, we isolated AML cells from leukemic *Slug*^{+/+} or *Slug*^{-/-} primary recipients and transplanted these cells into syngeneic-irradiated secondary CD45.1 recipients. *Slug*^{-/-} AML secondary recipients showed fewer GFP⁺ cells and leukemic blasts in peripheral blood (PB) (Supplemental Figure 5B, 5E). Consistent with these findings, other parameters of AML severity were also reduced, e.g., spleen size and weight, and PB white cell count (WCC) (Supplemental Figure 5F, 5G, 5D). Similar to our primary BM transplantation (Supplemental Figure 5C), the *Slug*^{+/+} group developed AML significantly faster than the *Slug*^{-/-} group (median survival, 62 days vs 86 days, respectively; $P < 0.01$). To validate these findings in other subtypes of AML, we transduced Lin⁻Sca-1⁺ HSPCs from *Slug*^{+/+} or *Slug*^{-/-} mice with retroviral NUP98-HoxA9 particles, and then performed colony-forming assay and *in vivo* leukemogenesis assay. Our data showed that *Slug* depletion suppressed colony formation *in vitro* and prolonged recipient survival (Supplemental Figure 6). Collectively, these data demonstrated that *Slug* deficiency prolonged survival and diminished AML expansion.

The frequency of LSCs is thought to be correlated with patient prognosis as well as leukemia progression in mice⁹. We further analyzed LSC frequency in *Slug*^{+/+} and *Slug*^{-/-} secondary recipients. The results showed that *Slug* deficiency had lower L-GMP frequency (Figure 2D, Supplemental Figure 7), suggesting that *Slug* might regulate the self-renewal of LSCs. Cell cycle analysis revealed that there were fewer S/G2/M phase *Slug*^{-/-} LSCs with a concordant increase in G0/G1 phases compared with *Slug*^{+/+} LSCs (Figure 2E). *Slug*^{-/-} LSCs also showed extensive apoptosis in comparison to *Slug*^{+/+} LSCs (Figure 2F). To directly evaluate the effect of *Slug* depletion on the frequency of leukemia stem/initiation cells (LSCs/LICs), we conducted limiting dilution assays. As expected, the estimated LSC/LIC frequency of the *Slug*^{-/-} group was significantly lower than that of the *Slug*^{+/+} group (1/132.1–1250 versus 1/11.7–122) (Figure 2G). Since the survival difference between *Slug*^{+/+} and *Slug*^{-/-} AML recipients may be in part due to homing efficiency, we determined homing capability of secondary transplanted *Slug*^{+/+} and *Slug*^{-/-} AML cells. The results showed that home efficiencies were similar between *Slug*^{+/+} and *Slug*^{-/-} AML cells at 16 h after BM transplantation (Figure 2H). Collectively, these data demonstrated that *Slug* deficiency impaired cell cycle and enhanced apoptosis in LSCs, thereby delaying AML progression *in vivo*.

Inhibition of endogenous *Slug* impairs self-renewal of MLL-AF9-derived LSCs

—To determine the functional significance of *Slug* in definitive LSCs, we knocked down *Slug* in MLL-AF9 driven-LSCs by lentivirus-expressing shRNAs. Our data showed that endogenous *Slug* was reduced 85% in LSCs by the two *Slug* shRNAs (Supplemental Figure 8A). Next, we performed colony-forming/replating assays using MLL-AF9-driven LSCs transduced with scrambled shRNA (control) and two *Slug* shRNAs, respectively. Knockdown of endogenous *Slug* significantly reduced colony numbers in comparison to the control group (Supplemental Figure 8B). Next, we transplanted an equal number of shRNA-transduced LSCs into irradiated CD45.1 recipient mice. After 3 weeks of transplantation, we analyzed AML cells in PB, spleen weight, LSC frequency, and cell cycle and apoptosis of LSCs. The results showed that inhibition of endogenous *Slug* decreased the frequency of GPF⁺ AML cells in PB and LSC frequency in BM compared with the control group (Supplemental Figure 8C-8E). Suppression of *Slug* expression also attenuated cell cycle and promoted apoptosis in a knockdown efficiency-dependent manner, consistent with the previous data (Supplemental Figure 8F, 8G). Notably, knockdown of *Slug* prolonged the survival of the recipient and delayed leukemia progression (median survival, 49 days in control group vs 58 and 61 days in two shRNA groups, respectively, $P < 0.01$) (Supplemental Figure 8H). These data demonstrated that inhibition of *Slug* expression significantly impaired self-renewal capacity of LSCs.

***Slc13a3* is a direct target of *Slug* in MLL-AF9-derived LSCs**—To gain insights into molecular mechanisms by which *Slug* regulates the self-renewal of LSCs, we sorted *Slug*^{+/+} and *Slug*^{-/-} MLL-AF9-driven LSCs from two groups of leukemic recipients. Next, we compared gene expression profiles in the two groups of LSCs by performing microarray analysis (Figure 3A). We found that 35 genes were upregulated, and 17 genes that were downregulated by >2.0-fold ($P < 0.05$) in *Slug*^{-/-} LSCs compared with *Slug*^{+/+} LSCs (Supplemental Table 5). Among the 52 *Slug*-regulated transcripts, some transcripts (e.g., *Erdr1*, *GPR84*, *Lcn2*, *Wap*, *Tbrg1*, *Slc2a5*, and *Elov17*) have been shown to play important roles in different types of cancer. Using real-time PCR, we validated our microarray results and confirmed that *Tbrg1*, *Erdr1*, and *Slc13a3* were upregulated, and *Slc2a5* and *Elov17* were repressed in *Slug*^{-/-} LSCs (Figure 3B). Since *Slug* mainly functions as a transcription repressor, we thus decided to focus on *Slc13a3* that is highly expressed in renal tissues. In order to search *Slug* binding sites in proximal promoter regions of *Slc13a3* (~1.0 kb from transcription start site), we performed promoter analysis using software INSECT2.0 and found two E-boxes (CAGGTG or CACCTG) as *Slug* binding sites (Figure 3C). Therefore, we decided to focus on *Slc13a3* as a potential target gene of *Slug* in regulation of LSCs. To determine whether *Slc13a3* is a true gene target of the *Slug* transcriptional repressor, we generated a luciferase reporter driven by the *Slc13a3* promoter (*Slc13a3*-Luc). Next, we performed luciferase reporter assays to validate our bioinformatics prediction by transfecting *Slc13a3* promoter reporter together with a *Slug* expression plasmid in 293T cells. Our data revealed that the *Slc13a3* luciferase reporter was inhibited 50% by *Slug* overexpression (Figure 3D). To test whether *Slug* could compete for occupancy at the E-boxes within promoter region of *Slc13a3* with other E-box binding transcription factors, we performed *Slc13a3* luciferase reporter assay by co-transfecting c-Myc expression vector with an increasing dose of *Slug* expression vector. The results showed that overexpression of *Slug*

did not affect transcription activation of c-Myc on *Slc13a3* luciferase reporter (Supplemental Figure 9). To examine whether *Slug* directly occupies the *Slc13a3* promoter, we overexpressed a Flag-tagged *Slug* in HSPCs using retrovirus and then performed ChIP assay using anti-Flag antibody. A pair of primers were designed to amplify the DNA fragment covering the two E-Boxes in *Slc13a3* promoter. As shown in Figure 3E and Supplemental Figure 10, a specific DNA fragment was amplified from the ChIP sample pulled down by the anti-Flag antibody but not by normal IgG control, indicating that *Slug* specifically binds to the *Slc13a3* promoter region *in vivo*. Our ChIP data indicates that *Slc13a3* is a direct transcriptional target of *Slug* in LSCs, hence a key question arises: does *Slug* regulate LSC self-renewal via *Slc13a3*? To this end, we generated lentiviral particles expressing scrambled shRNA (control) and four *Slc13a3* shRNAs (#1, #2, #3, and #4) were used to infect LSCs. As shown in Figure 3F, all *Slc13a3* shRNAs significantly knocked down the expression of endogenous *Slc13a3* in LSCs. Then, we performed *in vitro* colony-forming assay using LSCs expressing *Slc13a3* shRNA #1 and #3, respectively (Figure 3G). Our data showed that knockdown of *Slc13a3* rescued colony-forming capacity of *Slug*-deficient LSCs. Together, our findings demonstrated that *Slc13a3* is a direct functional target of *Slug* in LSCs.

***Slc13a3* overexpression delays the development of MLL-AF9-derived AML by *Slug*/ROS signaling**—Because *Slug* deficiency increased the expression of endogenous *Slc13a3*, we questioned whether forced expression of *Slc13a3* alone could impair AML development. To address this question, we overexpressed *Slc13a3* in LSCs by a retroviral vector. We showed that *Slc13a3* was moderately upregulated by 3.2-fold in retroviral vector expressing *Slc13a3* when compared to the normal kidney tissue (Supplemental Figure 11). Compared to the control group, overexpression of *Slc13a3* reduced colony numbers *in vitro* (Figure 4A). We transplanted an equal number of LSCs harboring retroviral vector only or overexpressing *Slc13a3* into irradiated recipient mice. Our flow-cytometric analysis showed that recipient mice transplanted with LSCs expressing *Slc13a3* exhibited much lower L-GMP frequency in BM at 16 weeks after transplantation (Figure 4B). Furthermore, overexpression of *Slc13a3* significantly delayed the progression of MLL-AF9-driven leukemia (Figure 4C). It has been reported that *Slc13a3* is a Na⁺/dicarboxylate cotransporter and it is associated with the Krebs cycle occurring in mitochondrial matrix for transporting several substrates, such as pyruvate, citrate, glutamine, and succinate²⁴. This would suggest that there is a possible link between *Slc13a3* and mitochondrial function. In AML cells, mitochondria generate ATP and consequently gives rise to intracellular ROS that are directly or indirectly involved in cell cycle regulation and apoptosis^{25, 26}. Therefore, we next sought to test whether forced-expression of *Slc13a3* affects ROS production. Mean fluorescence intensity (MFI) analysis showed that intracellular ROS level was elevated in LSCs-overexpressing *Slc13a3* (Figure 4D). Next, we examined the effect of endogenous *Slug* on the level of ROS in LSCs from the recipients of LSCs. As expected, depletion of endogenous *Slug* increased intracellular ROS levels in LSCs. Knockdown of *Slc13a3* reduced intracellular ROS levels in *Slug*^{-/-} LSCs (Figure 4E). Furthermore, we showed that forced-expression of *Slug* increased colony formation ability *in vitro* and downregulated the expression of endogenous *Slc13a3* in MLL-AF9-driven AML cells. In AML recipient mice forced-expression of *Slug* in LSCs showed higher GFP⁺ cells in peripheral blood (PB), higher frequency of L-GMP in BM, and decreased endogenous ROS level in LSC when

compared to the control group (Supplemental Figure 12). To further investigate whether Slug/Slc13a3 impaired LSCs by regulating intracellular ROS, we used the antioxidant N-acetyl-L-cysteine (NAC) to reduce ROS levels in the recipients. The results showed that NAC administration impaired functions of Slug and Slc13a3 on LSCs and leukemia progression (Figure 4F-4H, Supplemental Figure 13). In total, our data indicated that *Slug* functions as a negative regulator of the *Slc13a3*-ROS signaling pathway (Figure 4I).

Suppression of SLUG and forced-expressed SLC13A3 impairs human AMLs—

Although the results from the murine models provided robust evidence for a critical function of Slug and Slc13a3 on the establishment and maintenance of murine LSC induced by MLL-AF9, it was not clear whether SLUG and SLC13A3 also affects the development of human leukemia. To this end, we generated inducible lentiviral particles expressing scrambled shRNA (control) and two human SLUG shRNAs (#1 and #2). As shown in Supplemental Figure 14A, SLUG shRNA #1 and #2 reduced the expression of endogenous SLUG in human leukemia cells by 47% and 70% after induced by doxycycline, respectively. Next, we transduced the three shRNA-expressing lentiviral particles into five different human leukemic cell lines including THP-1 cells carrying t(9;11), MONOMAC-6 cells carrying t(9;11), NOMO-1 cells carrying t(9;11), MV4-11 cells carrying t(4;11), and NB4 cells carrying t(15;17). Stable infected leukemia cell lines were selected by puromycin following lentiviral infection and expanded for further studies. By performing cell growth/proliferation assay, we showed that inducible knockdown of SLUG inhibited the growth of all human leukemia cells (Supplemental Figure 14B–14F) with different inhibitory efficiencies. *In vitro* colony-forming assay revealed a reduced colony number in the groups with inducible knockdown of SLUG in comparison to scramble shRNA groups (Supplemental Figure 14G). To examine whether knockdown of *SLUG* impairs LSC self-renewal in human AML cells, we conducted long-term culture-initiating assay. The results showed the estimated LSC/LIC frequency of the SLUG-knockdown group was significantly lower than that of the control group (1/120.57–634.2 versus 1/4.11–25.2) (Supplemental Figure 14H). In addition, knockdown of *SLUG* elevated the mRNA and protein levels of SLC13A3 in human AML cells (Supplemental Figure 14I, 14J).

To investigate whether pharmacological targeting of SLUG could serve as a therapeutic strategy for treating AML, we designed TAT-SNAG, a cell-permeable peptide corresponding to the SNAG domain of SLUG and delivered it into several human leukemia cells (Supplemental Figure 15). Inhibition of human leukemia cell growth by this peptide was observed in all AML cells (Supplemental Figure 16A–16G). *In vitro* colony-forming assay revealed a reduced colony number in the TAT-SNAG groups in comparison to the control peptide treated groups (Supplemental Figure 16H). To further test whether TAT-SNAG peptide and standard chemotherapy drug could have synergistic effects on induction of cytotoxicity in AML cells, we treated human AML cells with cytarabine (Ara-C) and/or TAT-SNAG peptide. The results showed that TAT-SNAG peptide combined with Ara-C significantly suppressed the growth of human AML cell lines (Figure 5, Supplemental Figure 17).

To evaluate the roles of Slc13a3 in human AML cells, we first assessed potential clinical relevance of SLC13A3 expression levels in AML patients and in normal human population.

The results showed that SLC13A3 expression was obviously downregulated in peripheral blood cells of AML patients, BM mononuclear cells (MNCs) of FAB subtype AML-M1, M2, M3, M4, M5 versus normal blood cells and BM monocytes (Supplemental Figure 18A, 18B, Supplemental Table 2). SLC13A3 expression was also decreased in LSCs from AML patients compared to normal GMPs (Supplemental Figure 18C). Meanwhile, we observed a significant positive correlation between SLUG expression and SLC13A3 expression (Supplemental Figure 19A). In contrast, we did not observe any significant correlation between SNAIL1 or SNAIL3 (other SLUG/SNAIL family members) and SLC13A3, and the correlations of SLUG with KIT, FOXM1, c-MYC (Supplemental Figure 19B–19F). Of note, the correlation between SLUG and SLC13A3 expression was not particularly strong, which is expected since SLC13a3 is likely regulated by additional mechanisms.

Next, we explored functional potentials of SLC13A3 in human AML cells. Forced-expression of *Slc13a3* suppressed all human leukemia cell growth and reduced colony formation *in vitro* (Supplemental Figure 18D–18K). Collectively, these data demonstrate that SLUG and SLC13A3 is potential therapeutic targets for human AML.

DISCUSSION

AML is the first hematopoietic malignancy shown to be dependent on the LSC compartment²⁷. Similar to normal HSCs, LSCs reside at the apex of a hierarchy of malignant cells, and have the capacity to generate leukemia. The self-renewal and differentiation block are two key features of LSCs. Targeting LSCs for clinical AML therapy is a promising strategy for preventing AML relapse and improving long-term outcomes. Here, we revealed that *Slug* negatively regulates LSC self-renewal in part through its direct target *Slc13a3*, a sodium-dependent dicarboxylate transporter (NaDC3). Functional roles of *Slc13a3* in leukemogenesis have not previously been reported. But here, we observed that *Slug/Slc13a3* modulates LSC self-renewal by intracellular ROS. Either inhibition of *Slug* or forced-expression of *Slc13a3* is able to delay leukemia progression, suggesting that both *Slug* and *Slc13a3* are potential therapeutic targets of LSCs.

Slug is highly expressed in normal HSCs and involved in many important biological processes^{16–19, 22}. Previous studies have shown that either overexpression of *Slug* in mice induces mesenchymal tumors (leukemia and sarcomas) or SLUG gene-silencing inhibits the growth of specific leukemia cell lines^{21, 28}. Despite these descriptions of *Slug* in cancer development and leukemic cells, it has not been shown to the best of our knowledge that suppression of *Slug* not only delays the onset of AML and targets LSCs by regulation of the cell cycle and apoptosis *in vivo* and also negatively regulates the Krebs cycle's transporter *Slc13a3*.

It has been a challenge to identify specific therapeutic targets of LSCs, because LSCs appear to use self-renewal signaling pathways that are shared by normal HSCs²⁹. Current chemotherapy does not only kill leukemic cells but also impairs normal HSC functions. Therefore, the reasonable that targeting LSCs is not only capable of alleviating leukemia and enhancing the effect of chemotherapy, but is also able to protect and promote HSC regeneration after chemotherapy. Interestingly, our prior data showed that depletion of *Slug*

enhances the self-renewal of normal HSCs through a negative-feedback loop in SCF/c-Kit-Myc/FoxM1 signaling pathway during BM regeneration²². In our current study, we found that Slug has no effect on expression levels of c-Kit, c-Myc and FoxM1 in LSCs by microarray analysis (data not shown), no effect on expression of Slc13a3 and ROS levels in normal HSCs, and no significant correlations with KIT, FOXM1, and MYC in human AML patients. Our findings suggest that Slug regulates normal HSC and LSCs by distinct signaling pathways. Thus, taking those findings into account with the findings in the current study, we conclude that *Slug* is a potential target of LSCs for human AML therapy.

Slc13a3, a high-affinity sodium-dependent dicarboxylate cotransporter, belongs to the organic anion transmembrane transport protein family that is responsible for reabsorption or transport of Krebs cycle intermediates. *Slc13a3* is highly expressed in metabolically active tissues, such as in the kidney, liver and brain³⁰. Although its physiological significance is clear, the functional roles of *Slc13a3* in mammalian cells, especially in LSCs, have not been elucidated. Previous reports showed that Slc13a3 induces premature cellular senescence with decreasing ATP level in renal tubular cells³¹. In our present study, *Slug* deficiency reactivated the expression of endogenous *Slc13a3* in LSCs. Interestingly, overexpression of *Slc13a3* in MLL-AF9-driven LSCs prolongs the survival of recipient mice with a reduced frequency of LSCs. Thus, our data suggest that *Slc13a3* is a potential suppressor of AML initiation and development.

Since *Slc13a3* is involved in cellular energy metabolism, ectopic expression of Slc13a3 will inevitably consume more oxygen and produce more ROS. Our current microarray results also revealed that Slc2a5 and Elov17, two other cellular metabolic transcripts, were downregulated in *Slug*^{-/-} LSCs compared to *Slug*^{+/+} LSCs, suggesting both of the two genes are potential targets of Slug in LSCs. According to a recent study, Slc2a5 compensates for glucose deficiency in AMLs and may be linked to poor outcomes in AML patients³². *Elov17*, a long-chain fatty acid elongase, is highly expressed in prostate cancer cells associated with lipid metabolism³³. Knockdown of *Elov17* dramatically attenuates the growth of prostate cancer cells. Taking those results into account with our findings, we postulate that Slug likely regulates cellular metabolism through its main downstream targets Slc13a3, Slc2a5, and Elov17. Although there is no evidence elucidating the roles of Slug in normal HSC metabolism, the different functions of Slug on normal HSCs and LSCs implicates a different cellular metabolic signature between normal HSCs from that of LSCs.

Altogether, our current findings reveal a novel *Slug/Slc13a3* axis, which finely regulates an intracellular metabolic signaling pathway in LSCs. On the basis of our findings, pharmacological targeting of LSCs by either *Slug* or *Slc13a3*, together with chemotherapy, will be a highly effective strategy for improving outcomes in AML patients.

Supplementary Material

Refer to Web version on PubMed Central for supplementary material.

ACKNOWLEDGMENTS

This research was supported in part by an NIDDK/NIH grant (5R01DK090478–06). Z.Z. was supported by the Program for Professor of Special Appointment (Eastern Scholar) at Shanghai Institutions of Higher Learning, and the Natural Science Foundation of Shanghai (Grant No. 18ZR1414900). L.L was supported by a grant from the National Nature Science Foundation of China (No. 81500133)

References

1. Feng Z, Yao Y, Zhou C, Chen F, Wu F, Wei L, et al. Pharmacological inhibition of LSD1 for the treatment of MLL-rearranged leukemia. *J Hematol Oncol* 2016 3 12; 9: 24.
2. Szer J The prevalent predicament of relapsed acute myeloid leukemia. *Hematology Am Soc Hematol Educ Program* 2012; 2012: 43–48. [PubMed: 23233559]
3. Bruedigam C, Bagger FO, Heidel FH, Paine Kuhn C, Guignes S, Song A, et al. Telomerase inhibition effectively targets mouse and human AML stem cells and delays relapse following chemotherapy. *Cell Stem Cell* 2014 12 4; 15(6): 775–790. [PubMed: 25479751]
4. Chen CS, Sorensen PH, Domer PH, Reaman GH, Korsmeyer SJ, Heerema NA, et al. Molecular rearrangements on chromosome 11q23 predominate in infant acute lymphoblastic leukemia and are associated with specific biologic variables and poor outcome. *Blood* 1993 5 1; 81(9): 2386–2393. [PubMed: 8481519]
5. Hilden JM, Dinndorf PA, Meerbaum SO, Sather H, Villaluna D, Heerema NA, et al. Analysis of prognostic factors of acute lymphoblastic leukemia in infants: report on CCG 1953 from the Children's Oncology Group. *Blood* 2006 7 15; 108(2): 441–451. [PubMed: 16556894]
6. Mrozek K, Heinonen K, Lawrence D, Carroll AJ, Koduru PR, Rao KW, et al. Adult patients with de novo acute myeloid leukemia and t(9; 11)(p22; q23) have a superior outcome to patients with other translocations involving band 11q23: a cancer and leukemia group B study. *Blood* 1997 12 1; 90(11): 4532–4538. [PubMed: 9373264]
7. Krivtsov AV, Twomey D, Feng Z, Stubbs MC, Wang Y, Faber J, et al. Transformation from committed progenitor to leukaemia stem cell initiated by MLL-AF9. *Nature* 2006 8 17; 442(7104): 818–822. [PubMed: 16862118]
8. Huntly BJ, Shigematsu H, Deguchi K, Lee BH, Mizuno S, Duclos N, et al. MOZ-TIF2, but not BCR-ABL, confers properties of leukemic stem cells to committed murine hematopoietic progenitors. *Cancer Cell* 2004 12; 6(6): 587–596. [PubMed: 15607963]
9. Zheng Y, Zhang H, Wang Y, Li X, Lu P, Dong F, et al. Loss of Dnmt3b accelerates MLL-AF9 leukemia progression. *Leukemia* 2016 12; 30(12): 2373–2384. [PubMed: 27133822]
10. Huret JL, Dessen P, Bernheim A. An atlas of chromosomes in hematological malignancies. Example: 11q23 and MLL partners. *Leukemia* 2001 6; 15(6): 987–989. [PubMed: 11417488]
11. Brabletz T EMT and MET in metastasis: where are the cancer stem cells? *Cancer Cell* 2012 12 11; 22(6): 699–701. [PubMed: 23238008]
12. Gessner A, Thomas M, Castro PG, Buchler L, Scholz A, Brummendorf TH, et al. Leukemic fusion genes MLL/AF4 and AML1/MTG8 support leukemic self-renewal by controlling expression of the telomerase subunit TERT. *Leukemia* 2010 10; 24(10): 1751–1759. [PubMed: 20686504]
13. Yilmaz OH, Valdez R, Theisen BK, Guo W, Ferguson DO, Wu H, et al. Pten dependence distinguishes haematopoietic stem cells from leukaemia-initiating cells. *Nature* 2006 5 25; 441(7092): 475–482. [PubMed: 16598206]
14. Guzman ML, Neering SJ, Upchurch D, Grimes B, Howard DS, Rizzieri DA, et al. Nuclear factor-kappaB is constitutively activated in primitive human acute myelogenous leukemia cells. *Blood* 2001 10 15; 98(8): 2301–2307. [PubMed: 11588023]
15. Sun Y, Shao L, Bai H, Wang ZZ, Wu WS. Slug deficiency enhances self-renewal of hematopoietic stem cells during hematopoietic regeneration. *Blood* 2010 3 4; 115(9): 1709–1717. [PubMed: 20032500]
16. Shih JY, Yang PC. The EMT regulator slug and lung carcinogenesis. *Carcinogenesis* 2011 9; 32(9): 1299–1304. [PubMed: 21665887]

17. Phillips S, Prat A, Sedic M, Proia T, Wronski A, Mazumdar S, et al. Cell-state transitions regulated by SLUG are critical for tissue regeneration and tumor initiation. *Stem Cell Reports* 2014 5 6; 2(5): 633–647. [PubMed: 24936451]
18. Wang SP, Wang WL, Chang YL, Wu CT, Chao YC, Kao SH, et al. p53 controls cancer cell invasion by inducing the MDM2-mediated degradation of Slug. *Nat Cell Biol* 2009 6; 11(6): 694–704. [PubMed: 19448627]
19. Liu X, Sun H, Qi J, Wang L, He S, Liu J, et al. Sequential introduction of reprogramming factors reveals a time-sensitive requirement for individual factors and a sequential EMT-MET mechanism for optimal reprogramming. *Nat Cell Biol* 2013 7; 15(7): 829–838. [PubMed: 23708003]
20. Inukai T, Inoue A, Kurosawa H, Goi K, Shinjyo T, Ozawa K, et al. SLUG, a ces-1-related zinc finger transcription factor gene with antiapoptotic activity, is a downstream target of the E2A-HLF oncoprotein. *Mol Cell* 1999 9; 4(3): 343–352. [PubMed: 10518215]
21. Perez-Mancera PA, Gonzalez-Herrero I, Perez-Caro M, Gutierrez-Cianca N, Flores T, Gutierrez-Adan A, et al. SLUG in cancer development. *Oncogene* 2005 4 28; 24(19): 3073–3082. [PubMed: 15735690]
22. Zhang Z, Zhu P, Zhou Y, Sheng Y, Hong Y, Xiang D, et al. A novel slug-containing negative-feedback loop regulates SCF/c-Kit-mediated hematopoietic stem cell self-renewal. *Leukemia* 2017 2; 31(2): 403–413. [PubMed: 27451973]
23. Zhang CC, Kaba M, Ge G, Xie K, Tong W, Hug C, et al. Angiopoietin-like proteins stimulate ex vivo expansion of hematopoietic stem cells. *Nat Med* 2006 2; 12(2): 240–245. [PubMed: 16429146]
24. Pajor AM, Gangula R, Yao X. Cloning and functional characterization of a high-affinity Na(+)/dicarboxylate cotransporter from mouse brain. *Am J Physiol Cell Physiol* 2001 5; 280(5): C1215–1223. [PubMed: 11287335]
25. Hole PS, Zabkiewicz J, Munje C, Newton Z, Pearn L, White P, et al. Overproduction of NOX-derived ROS in AML promotes proliferation and is associated with defective oxidative stress signaling. *Blood* 2013 11 7; 122(19): 3322–3330. [PubMed: 24089327]
26. Paul TA, Bies J, Small D, Wolff L. Signatures of polycomb repression and reduced H3K4 trimethylation are associated with p15INK4b DNA methylation in AML. *Blood* 2010 4 15; 115(15): 3098–3108. [PubMed: 20190193]
27. Chan WI, Huntly BJ. Leukemia stem cells in acute myeloid leukemia. *Semin Oncol* 2008 8; 35(4): 326–335. [PubMed: 18692683]
28. Wei CR, Liu J, Yu XJ. Targeting SLUG sensitizes leukemia cells to ADR-induced apoptosis. *Int J Clin Exp Med* 2015; 8(12): 22139–22148. [PubMed: 26885188]
29. Lataillade JJ, Pierre-Louis O, Hasselbalch HC, Uzan G, Jasmin C, Martyre MC, et al. Does primary myelofibrosis involve a defective stem cell niche? From concept to evidence. *Blood* 2008 10 15; 112(8): 3026–3035. [PubMed: 18669872]
30. Chen X, Tsukaguchi H, Chen XZ, Berger UV, Hediger MA. Molecular and functional analysis of SDCT2, a novel rat sodium-dependent dicarboxylate transporter. *J Clin Invest* 1999 4; 103(8): 1159–1168. [PubMed: 10207168]
31. Ma Y, Bai XY, Du X, Fu B, Chen X. NaDC3 Induces Premature Cellular Senescence by Promoting Transport of Krebs Cycle Intermediates, Increasing NADH, and Exacerbating Oxidative Damage. *J Gerontol A Biol Sci Med Sci* 2016 1; 71(1): 1–12. [PubMed: 25384549]
32. Chen WL, Wang YY, Zhao A, Xia L, Xie G, Su M, et al. Enhanced Fructose Utilization Mediated by SLC2A5 Is a Unique Metabolic Feature of Acute Myeloid Leukemia with Therapeutic Potential. *Cancer Cell* 2016 11 14; 30(5): 779–791. [PubMed: 27746145]
33. Tamura K, Makino A, Hullin-Matsuda F, Kobayashi T, Furihata M, Chung S, et al. Novel lipogenic enzyme ELOVL7 is involved in prostate cancer growth through saturated long-chain fatty acid metabolism. *Cancer Res* 2009 10 15; 69(20): 8133–8140. [PubMed: 19826053]
34. Perez-Losada J, Sanchez-Martin M, Rodriguez-Garcia A, Sanchez ML, Orfao A, Flores T, et al. Zinc-finger transcription factor Slug contributes to the function of the stem cell factor c-kit signaling pathway. *Blood* 2002 8 15; 100(4): 1274–1286. [PubMed: 12149208]

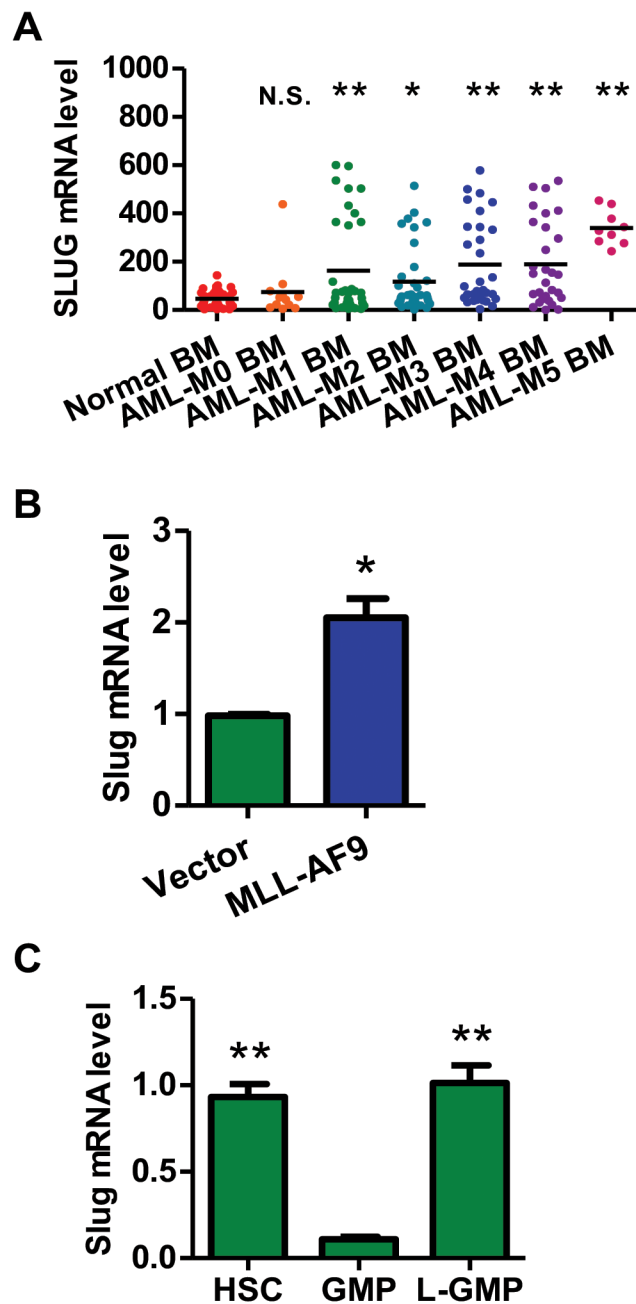


Figure 1. *Slug* is highly expressed in both human and mouse AML cells.

(A) The expression of SLUG between normal bone marrow cells of healthy controls and FAB subtypes of AML patients. The data were obtained from a public microarray database (GSE15061, GSE11504, GSE19429, and GSE10358) (normal patient, n = 111; M0 patient n = 12; M1 patient n = 35; M2 patient n = 36; M3 patient n = 31; M4 patient n = 29; M5 patient n = 9).

(B) qPCR analysis of the expression of endogenous *Slug* in mouse HSPCs transduced with retroviral vector only or retrovirus expressing MLL-AF9. Results are normalized to *Gapdh* expression and expressed relative to *Slug* expression in vector group (n = 3).

(C) qPCR analysis of the expression level of *Slug* in mouse HSCs, GMP and LSC. The indicated cells were sorted by flow cytometry. HSC: Lin⁻Sca-1⁺c-Kit⁺CD150⁺CD48⁻, GMP: Lin⁻c-Kit⁺CD34⁺CD16/32⁺, LSC (L-GMP): GFP⁺Lin^{low}c-Kit⁺CD34⁺CD16/32⁺ (n = 3). Results are normalized to *Hprt* expression and expressed relative to *Slug* expression in GMP group (n = 3).

Data are representative of two to three independent experiments. All data are represented as mean ± SD. Two-tailed Student's *t*-test were used to assess statistical significance (* *P* < 0.05; ** *P* < 0.01). See also Supplemental Figure 1, 2, and 3.

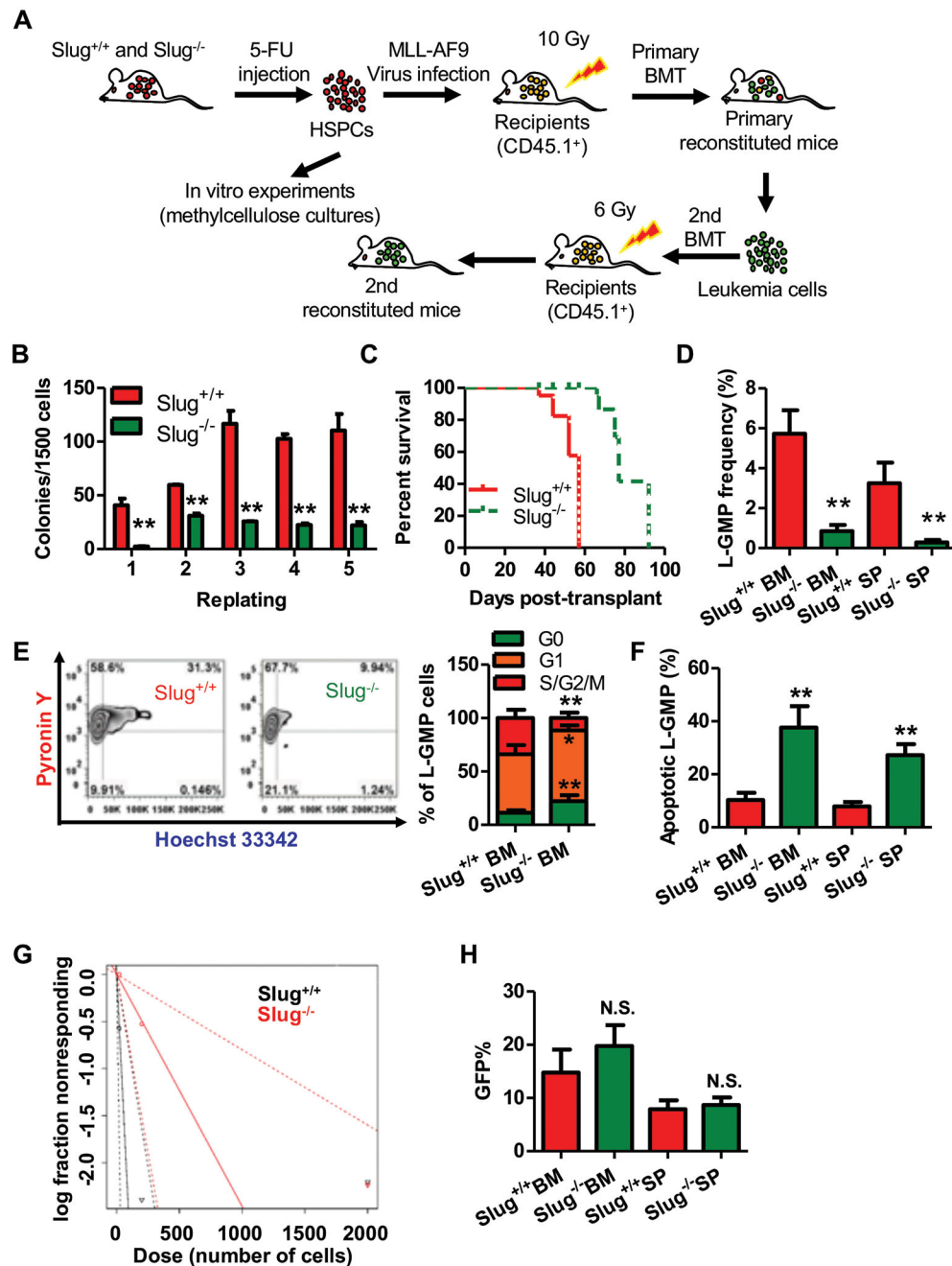


Figure 2. *Slug* deficiency impairs self-renewal of LSCs and delays MLL-AF9 leukemia onset. (A) Experimental schema of MLL-AF9-driven AML. BMCs were isolated from *Slug*^{+/+} or *Slug*^{-/-} mice treated with 150 mg 5-FU/kg BW for 6 days, transduced with MLL-AF9 retrovirus *in vitro* in order to generate AML cells, and transplanted into irradiated recipient mice (CD45.1). For primary transplantation, 1X10³ GFP⁺ cells were injected. For secondary transplantation, 5X10⁵ or 5X10⁴ GFP⁺ cells were injected. (B) Colony-forming assay of *Slug*^{+/+} or *Slug*^{-/-} AML cells (n = 3).

(C) Survival analysis of primary recipient mice. Median survival was 57 versus 77 days post-transplant for primary recipients of *Slug*^{+/+} or *Slug*^{-/-} AML cells, respectively ($P < 0.01$, Mantel-Cox test; $n = 5$).

(D) Frequency of L-GMP in the BM and spleen (SP) from secondary recipients injected with 5×10^4 *Slug*^{+/+} or *Slug*^{-/-} AML cells at week 7 post-transplantation ($n = 4$).

(E) Cell cycle phase distribution of L-GMP cells in BM from secondary recipients injected with 5×10^4 *Slug*^{+/+} or *Slug*^{-/-} AML cells at week 7 post-transplantation ($n = 4$).

(F) Percentage of apoptotic L-GMP cells in the BM and SP from secondary recipients injected with 5×10^4 *Slug*^{+/+} or *Slug*^{-/-} AML cells at week 7 post-transplantation ($n = 4$).

(G) Limiting dilution assay of *Slug*^{+/+} and *Slug*^{-/-} LSCs from secondary transplantation recipients. LSC/LICs frequencies calculated by ELDA software ($n = 5$).

(H) Quantification of homing AML cells at 16 h after transplantation of GFP⁺ gated AML cells from secondary recipients ($n = 5$).

Data are representative of two to three independent experiments. Excluding survival analysis, all data are represented as mean \pm SD. Two-tailed Student's t-tests were used to assess statistical significance (* $P < 0.05$; ** $P < 0.01$). See also Supplemental Figure 4, 5, and 7.

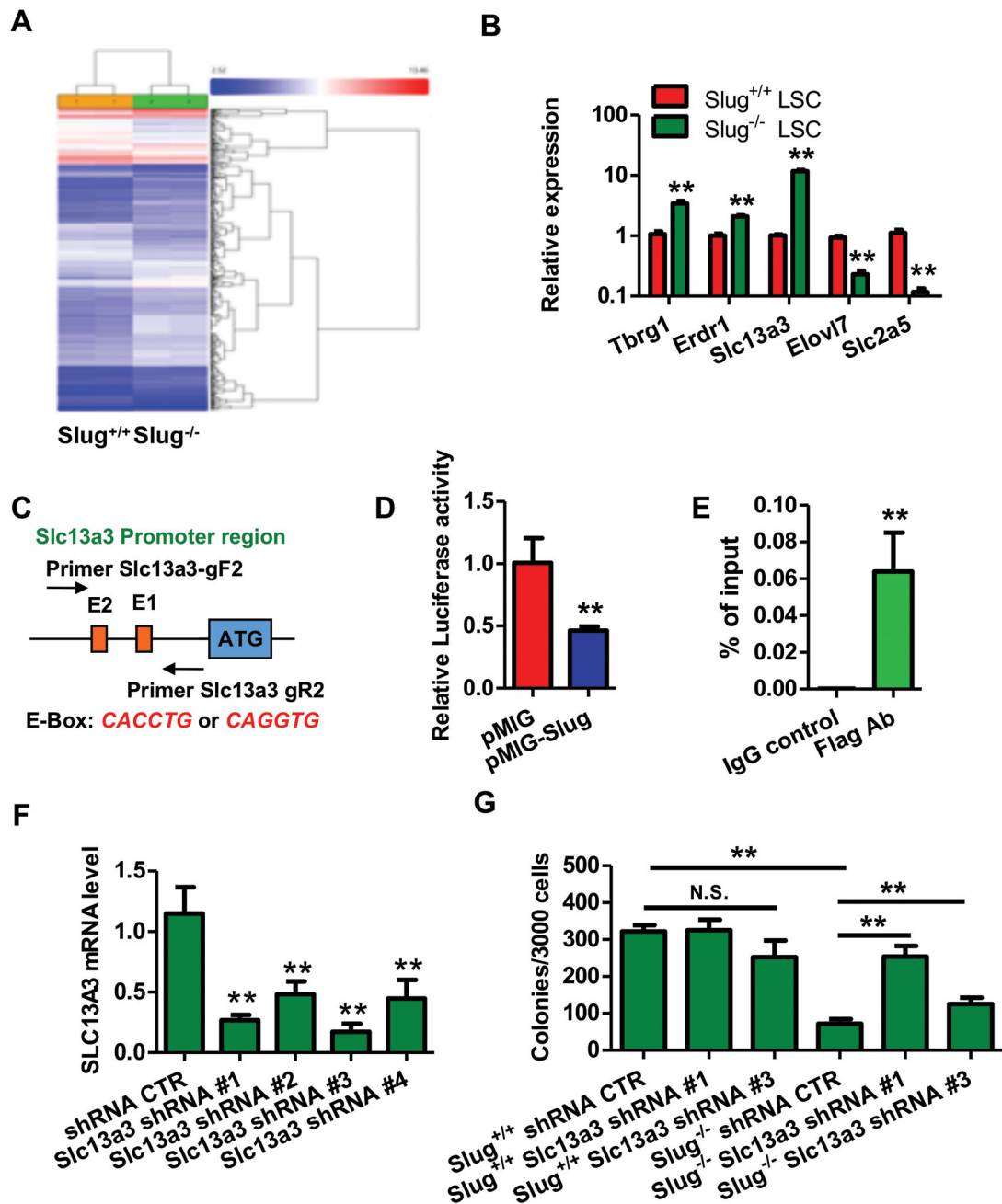


Figure 3. Gene profiling using microarray analysis identifies *Slug* potential targets in L-GMP cells during MLL-AF9-derived leukemia development.

(A) Microarray analysis of gene expression profiles in L-GMP cells sorted from the secondary recipient mice transplanted with *Slug*^{+/+} or *Slug*^{-/-} L-GMP cells (n = 2). The data were analyzed by ANOVA test.

(B) qPCR analysis of candidate target gene in L-GMP cells sorted from recipient mice transplanted with *Slug*^{+/+} or *Slug*^{-/-} AML cells (n = 3). Results are normalized to *Hprt* expression and expressed relative to expression of target genes in *Slug*^{+/+} L-GMPs (n = 3).

(C) Diagram of E-Box for the *Slc13a3* promoter.

(D) Slc13a3 luciferase reporter assays. 293T cells were transfected with Slc13a3-Luc together with pMIG (vector control) or pMIG-Slug, then cultured for 72 h before luciferase activity assay. pCMV-LacZ was included in each transfection as an internal control to normalized luciferase activity (n = 3).

(E) Analysis of *Slug* occupancy at the *Slc13a3* promoter by ChIP-qPCR. qPCR was repeated three times.

(F) qPCR analysis of *Slc13a3* knockdown in AML cells. Results are normalized to *Hprt* expression and expressed relative to *Slc13a3* expression in shRNA CTR group (n = 3).

(G) Knockdown of Slc13a3 in part impaired the suppressive function of *Slug* on LSCs (n = 3).

Data are representative of two to three independent experiments. All data are represented as mean \pm SD. Two-tailed Student's t-tests were used to assess statistical significance (* $P < 0.05$; ** $P < 0.01$).

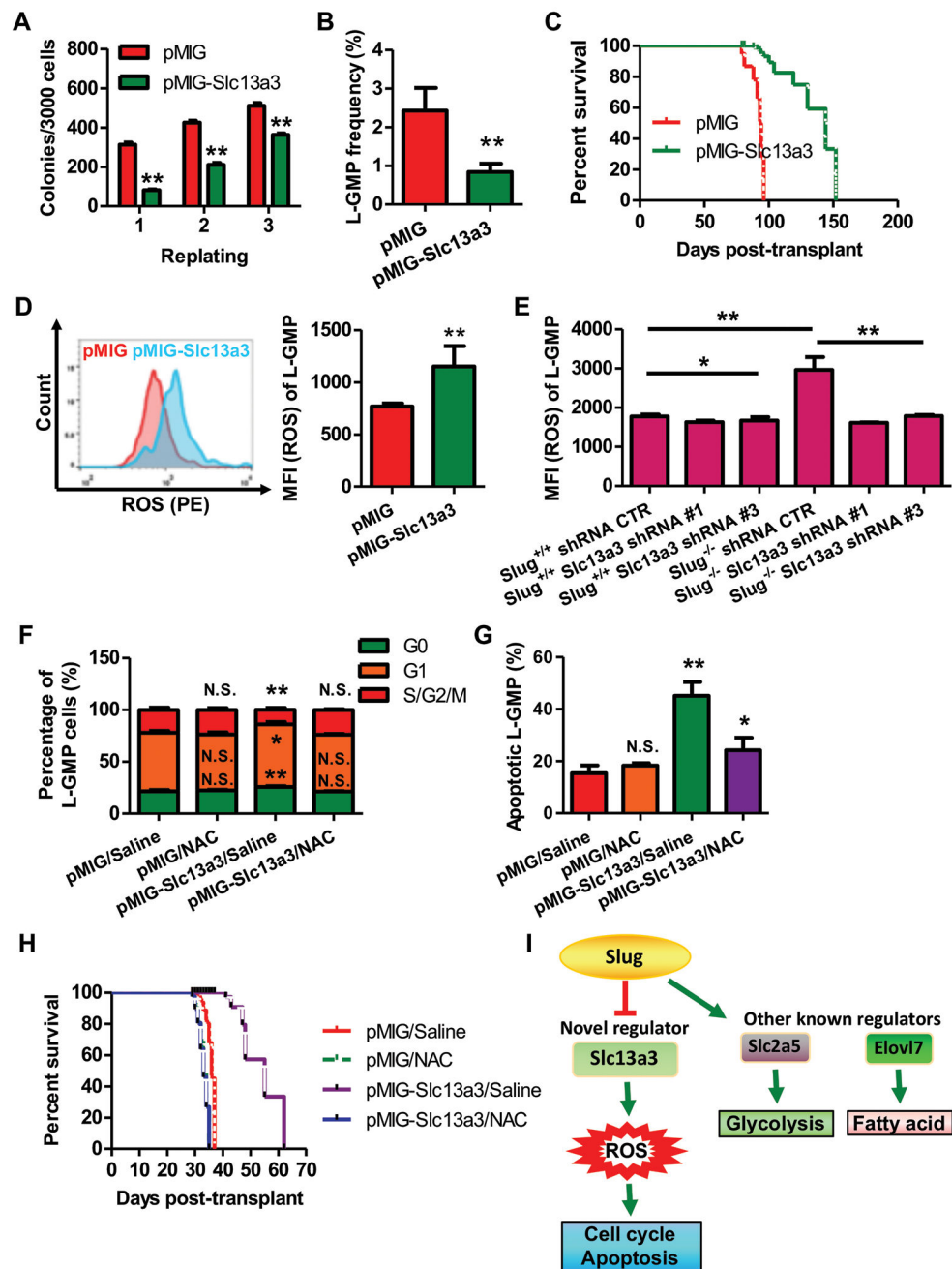


Figure 4. Overexpression of Slc13a3 diminishes self-renewal of MLL-AF9-derived LSCs by increasing ROS production.

(A) Colony-forming assay of AML cells by forced-expression of *Slc13a3* (n = 3).

(B) Frequency of L-GMP in the BM from primary recipients injected with 2×10^4 AML cells infected with retroviral vector pMIG and pMIG-Slc13a3, respectively, at week 16 post-transplantation (n = 4).

(C) Survival analysis of primary recipients injected with AML cells carrying pMIG vector or pMIG-Slc13a3. Median survival was 96 versus 144 days post-transplant for recipients of

2X10⁴ AML cells infected by pMIG vector and pMIG-Slc13a3, respectively ($P < 0.01$, Mantel-Cox test; n = 8).

(D) Flow cytometric analysis of ROS levels in L-GMPs from recipient mice injected with 2X10⁴ AML cells carrying pMIG vector and pMIG-Slc13a3, respectively. Levels of ROS were evaluated by flow cytometry. MFI, median fluorescence intensity (n = 4).

(E) Effects of endogenous Slc13a3 on ROS level in LSCs with or without *Slug* gene. L-GMPs were harvested from recipient mice injected with *Slug*^{+/+} and *Slug*^{-/-} AML cells expressing scramble shRNA, Slc13a3 shRNA #1 and #3, respectively. Levels of ROS were evaluated by flow cytometry (n = 5).

(F) Cell cycle phase distribution of L-GMP cells in BM from recipients injected with AML cells carrying pMIG or pMIG-Slc13a3 after treatment with saline or NAC (n = 4).

(G) Percentage of apoptotic L-GMP cells in BM from recipients receiving AML cells infected with pMIG or pMIG-Slc13a3 following treatment with saline or NAC (n = 4).

(H) Survival analysis of recipient mice receiving AMLs carrying retroviral vector pMIG or pMIG-Slc13a3 after treatment with saline or NAC. Median survival was 36, 33, 55, and 33 days post-transplant for recipients of AMLs infected with retroviral vectors pMIG or pMIG-Slc13a3, following treatment with saline or NAC, respectively ($P < 0.05$, Mantel-Cox test; n = 6).

(I) Action model of the *Slug/Slc13a3/ROS* cellular metabolic signaling pathway.

Data are representative of two to three independent experiments. All data are represented as mean \pm SD. Two-tailed Student's t-tests were used to assess statistical significance (* $P < 0.05$; ** $P < 0.01$). See also Supplemental Figure 13.

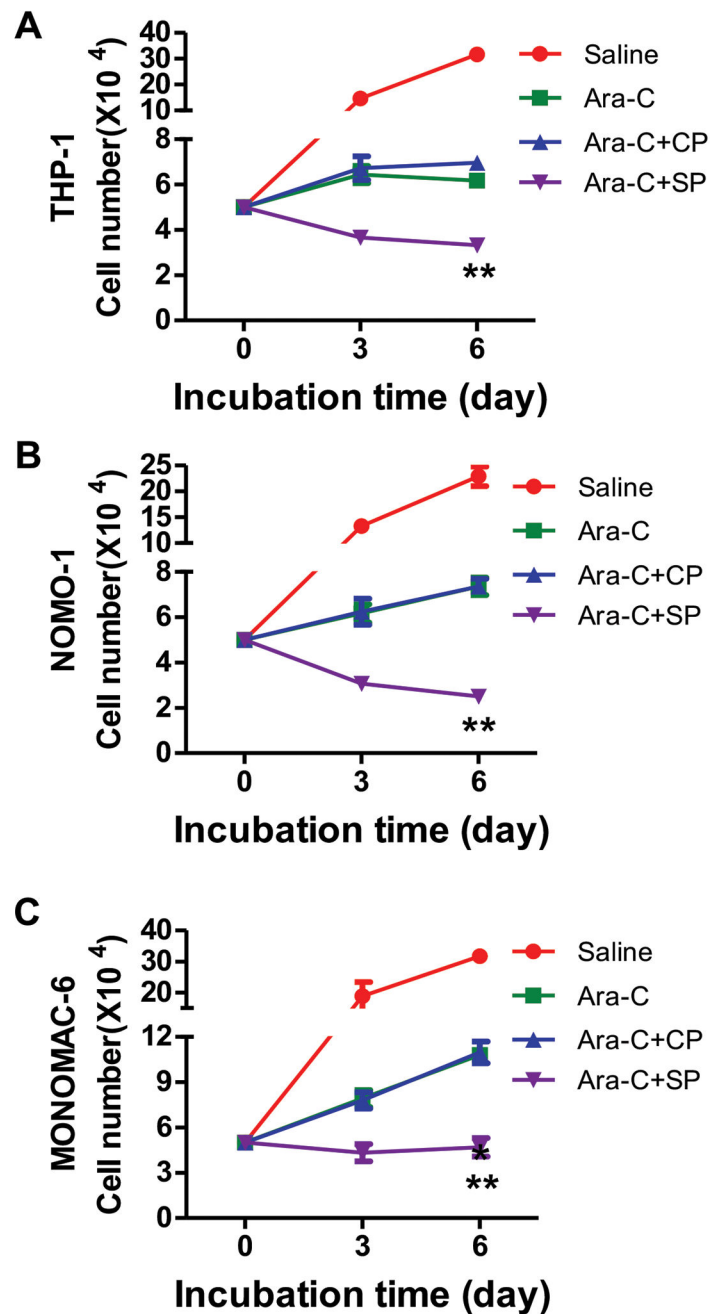


Figure 5. Enhancement of the cytotoxic effects of cytarabine in synergism with TAT-SNAG peptide in human AML cells.

(A-C) The growth of human AML cells after different treatments. The cells were cultured in RPMI1640 containing 10% fetal bovine serum treated with saline alone, cytarabine alone, the combination of cytarabine and control peptide (CP), or the combination of cytarabine and TAT-SNAG peptide (SP). The cell number was counted at different time points (n = 3). (A) THP-1, (B) NOMO-1, (C) NOMOMAC-6.

Data are representative of three independent experiments. All data are represented as mean \pm SD. Two-tailed Student's t-tests were used to assess statistical significance (** $P < 0.01$). See also Supplemental Figure 17.

Author Manuscript

Author Manuscript

Author Manuscript

Author Manuscript